

OPERATIONAL SPACE OF A SHAPED DIVERTOR IN ITER

A. S. Kukushkin, H. D. Pacher^a, G. Janeschitz, A. Loarte^b, D. Coster^c, D. Reiter^d

ITER Joint Central Team, Garching Joint Work Site, Garching, Germany,

^a INRS-Energie et Matériaux, Varennes, Québec, Canada, ^b EFDA CSU, Garching, Germany; ^c Max-Planck IPP, Garching, Germany; ^d FZ Jülich, Jülich, Germany

Design studies performed for ITER, mostly for a straight vertical target divertor geometry, have revealed that peak power loads are reduced when the targets meet the divertor bottom at an angle, forming a V-shape near the strike points [1, 2]. In this paper, a more detailed investigation of the divertor operational space is presented for the reference ITER V-shaped target (Fig. 1), with a realistic gas conductance between the inner and outer divertors taken into account. The conditions of modelling with the B2-Eirene code package are similar to those in [1, 2] except that here the DT ion flux from the core plasma is kept constant at $17 \text{ Pa}\cdot\text{m}^3/\text{s}$, representing deep core fuelling, and the rate of gas puffing from the top is varied to scan the density. The impurities are carbon sputtered from the targets, and helium, without additional impurity seeding. The operational space is presented in terms of separatrix plasma density in the outer mid-plane n_s , peak power on the targets q_{pk} , DT particle throughput Γ_{DT} , average He concentration at the separatrix c_{He} , DT puffing rate $\Gamma_{DT \text{ puff}}$ and DT atom influx into the core across the separatrix Γ_{DTos} . The most important limitations on the ITER operational window are $q_{pk} \leq 10 \text{ MW}/\text{m}^2$, $c_{He} \leq 0.06$, $\Gamma_{DT} \leq 200 \text{ Pa}\cdot\text{m}^3/\text{s}$ [1].

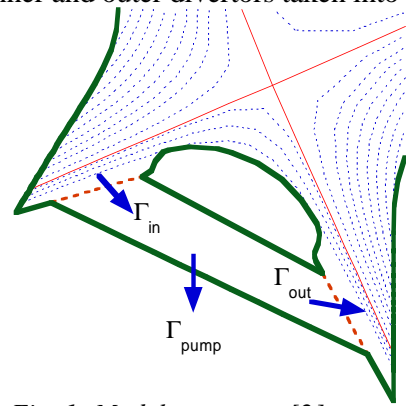


Fig. 1. Model geometry [2] corresponding to the reference ITER divertor. Thick dashed lines show the semi-transparent liner surfaces and arrows indicate a typical neutral flow pattern.

Inductive operation. ITER operation curves are presented in Fig. 2 for one value of pumping speed, $S_p = 20 \text{ m}^3/\text{s}$, for three values of the input power P_{in} (different assumptions on the fusion power and gain factor Q), as well as for four different values of S_p for $P_{in} = 100 \text{ MW}$. An operational window of reasonable size is seen to exist within these limits for a range of P_{in} , provided that n_s above $\sim 0.3 \cdot 10^{20} \text{ m}^{-3}$ is acceptable. The density increases and then is found to

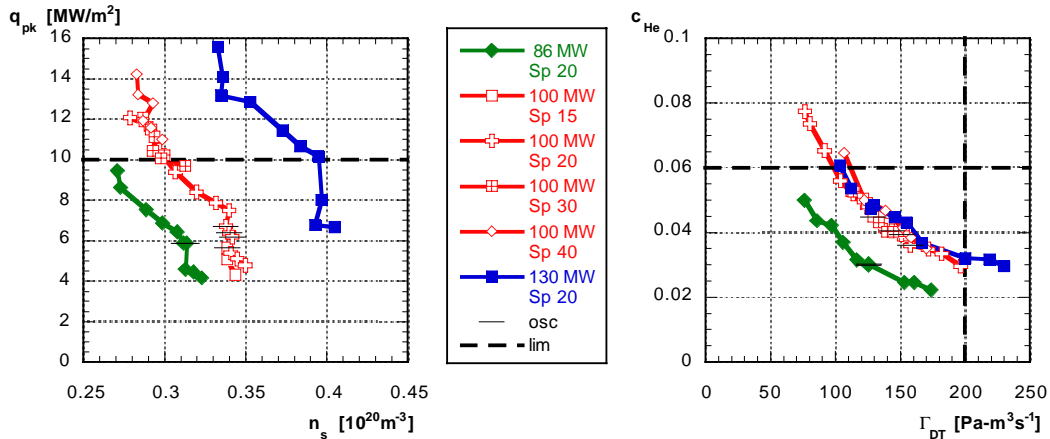


Fig. 2. Peak power loading vs. upstream plasma density and average helium concentration at the separatrix vs. DT particle throughput for different input power and pumping speed. Points corresponding to the divertor oscillations are marked with horizontal bars and limits are dashed.

saturate as Γ_{DT_puff} is increased (Fig. 3), accompanied by plasma detachment in the inner divertor. A further substantial increase of Γ_{DT_puff} leads again to an increase of n_s , with the inner divertor now fully detached. The saturation level, both in n_s and throughput, increases with input power, and the rate of increase with Γ_{DT_puff} of the recombination neutral source and of the power radiated by neutrals, increases where the density is saturated. This picture looks qualitatively similar to [3] where a theoretical model was developed which describes the saturation of n_s due to volume recombination. In that simplified model, only one divertor was considered, whereas in our case, it is the inner divertor, which carries the smaller part of the power and detaches first, that determines the effect. Because the outer divertor remains attached, a further density increase can occur once the detachment of the inner divertor is completed.

Other non-linear effects. The non-monotonic shape of some curves on the low-density side of Figs. 2 and 3 implies that a bifurcation of n_s can exist at the lower densities, at least for the higher input powers. Similar effects have also been seen in other studies (e.g. [4]). Furthermore, self-sustained oscillations in the divertor plasma [5] caused by a loss of neutral pressure balance across the magnetic field, appear in certain regions of the power-density space. The oscillations lead to some 20% modulation of the peak power load (the data in Fig. 2 are time-averaged). We do not see these oscillations for 130 MW, but have not yet explored the higher densities there.

Compatibility with the core. In all our previous analyses [1] we have investigated mostly the lower values of n_s because the available experimental data in H-mode indicated that n_s is not expected to exceed 1/3 to 1/4 of the line average density. For these conditions, our studies show that the atomic DT flux across the separatrix increases but weakly with Γ_{DT_puff} , staying almost constant for the high input power, Fig. 4. The scrape-off layer (SOL) plasma screens the core from both the puffed and the recycled neutrals. The gas puff is therefore a means of controlling the SOL and divertor density rather than the core density. Recent studies of core transport for ITER [6] have indicated the need to control the core fuelling intensity and profile. The present results indicate that a significant part of this control will have to be performed via deep fuelling (e.g. pellets, low-energy beams).

Non-inductive current drive. In this mode of operation, the plasma density, plasma current, and fusion power are reduced. The input power to the SOL (alpha plus auxiliary minus radiation)

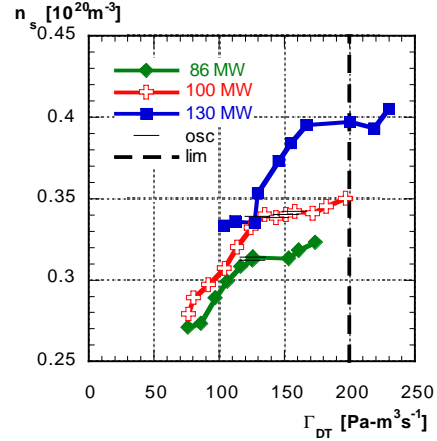


Fig. 3. Upstream plasma density vs. DT particle throughput for $S_p = 20 \text{ m}^3/\text{s}$ and different values of the input power.

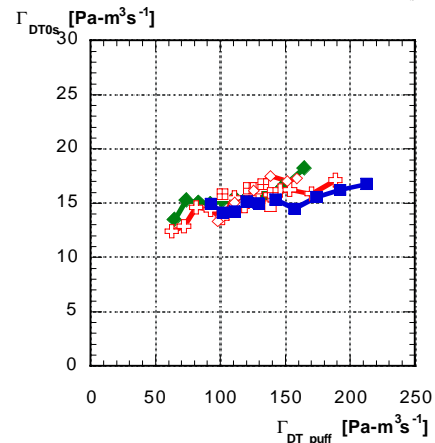


Fig. 4. DT atom influx into the core vs. gas puffing rate. For notations, see the legend in Fig. 2.

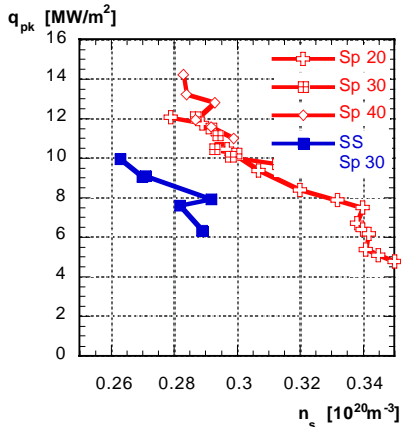


Fig. 5. Peak power vs. upstream density for steady-state operation (non-inductive current drive). The curves for inductive operation are also shown for comparison. $P_{in} = 100$ MW.

Target inclination. If it were possible to provide a stronger target inclination, both the peak power load in normal operation and the erosion due to type I ELMs would be reduced. In order to address the issue, we have studied the configuration shown in Fig. 6. If there were a strong increase of particle recycling on the upper part of the target, a change of core density profile and energy confinement could result. However, the modelling results indicate that, although the particle flux increases there, its value remains low and no noticeable change of the plasma profiles around the x-point is seen. The peak power loading is down by 30%, less than the 50% reduction of the angle between target and separatrix. A substantial part of the peak power is provided by radiation, which is found not to change with the angle, thus providing a smaller reduction of peak power. Such an alternative configuration might therefore be a way to mitigate the peak power and ELM erosion situation, at the cost of reducing the configuration flexibility, already

restricted by the requirement that the separatrix strike points be near the corners of the targets.

Position control. In order to see how these results would be affected by a variation of the x-point location within the control range provided by the equilibrium control system, a short series of runs was done for which the whole divertor was shifted down and to the left by 2 cm, the worst case for outer strike point movement. The power loading increased by about 10%.

Issues in impurity modelling. In the present model, the carbon particles are absorbed at every surface encountered. Carbon emission from non-carbon surfaces which would be in net erosion conditions, or in net redeposition conditions at significant sputtering levels, is therefore not modelled. This would certainly change the carbon flow patterns and can affect the predictions of the ITER divertor performance. First exploratory runs in a model with a tungsten “dome” which does not absorb carbon were carried out. They exhibit practically unchanged helium concentration and some 20% reduction of the peak power, so that further work in this direction

stays approximately the same (lower Q). The reduction of the plasma current ($q_{95} \cong 4.5$ instead of 3) increases the connection length, and this requires lower n_s for the same divertor plasma parameters. Indeed, longer connection means higher temperature upstream, with a correspondingly lower density because of pressure balance. The initial modelling results, shown in Fig. 5, confirm this trend: the limiting value of $q_{nk} = 10$ MW/m² is reached at $n_s \cong 0.26 \cdot 10^{20} \text{m}^{-3}$, a 15% reduction. The helium concentration stays low because of significantly lower fusion power.

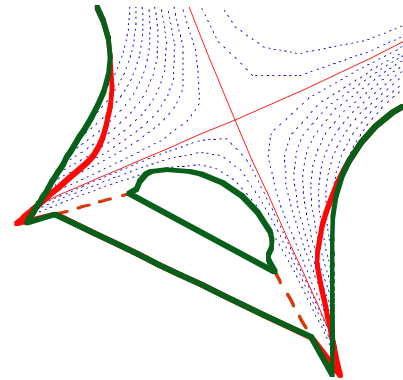


Fig. 6. The model geometry used for analysis of the effect of target inclination. The angle of the target surfaces to the separatrix reduced by a factor 2 (light or red) vs. the geometry of Fig. 1 (dark or green)

is required.

Furthermore, the present model does not include scattering of impurity atoms in the edge, in particular elastic collisions with the plasma ions. This is especially important for the helium atoms which have a high ionisation potential and therefore remain neutral longer than other impurities. First simulations with this effect included have shown a very substantial reduction of helium concentration, by a factor 2 to 4 depending on divertor geometry. The elastic collisions both heat up the He atoms, thus increasing their mean-free-path, and scatter them in angle, increasing the probability of reaching the pumping duct.

Conclusions.

The V-shaped target geometry in ITER offers a reasonable window for divertor operation in the primary operational mode relying on inductive current drive. The non-linear nature of the plasma transport in the edge produces a saturation of the separatrix density as a function of the puffing rate which accompanies the transition of the plasma in the inner divertor from the partially attached to the fully detached state. This saturation is overcome at higher puffing rates. Non-linear effects can also cause oscillations in the divertor plasma which lead to 20% modulation of the peak power loading on the targets. The core fuelling efficiency of gas puffing in ITER is expected to be low, varying from 20% to below 10% with the increase of the puffing rate. The dependence of the core neutral flux on density (puffing rate), and power is weak. Variation of the gas puffing rate changes DT throughput and controls mainly the helium concentration and divertor density, but control of the core plasma density profile would have to be provided by some means of direct core fuelling, such as pellets or beams. Non-inductive current drive operation corresponds to higher connection length, which shifts the operational window in the separatrix density down by 15%. Divertor operation in a back-up geometry with smaller target angle is found to yield acceptable results, However, although this would have the advantage of mitigating type I ELM erosion, the flexibility of the machine for configuration changes would be significantly reduced, so that the reference geometry is maintained. The variation of divertor parameters with plasma position within the control window is acceptably small for the reference V-shaped divertor. Initial calculations with improved impurity models, for both carbon and helium, have been carried out. A continuation of these studies, accompanied by studies of impurity seeding and divertor geometry optimisation, and an assessment of the impact on the predicted divertor performance, has become the priority issue for the near future.

This report has been prepared as an account of work undertaken within the framework of the ITER EDA Agreement. The views and opinions expressed herein do not necessarily reflect those of the Parties to the ITER Agreement, the IAEA or any agency thereof. Dissemination of the information in this paper is governed by the applicable terms of the ITER EDA Agreement.

- [1] A. S. Kukushkin et al., J. Nucl. Mater. **290–293** (2001) 887
- [2] A. S. Kukushkin, et al., 18th IAEA Fusion Conference, Sorrento, 2000
- [3] S. I. Krasheninnikov, et al., J. Nucl. Mater. **266–269** (1999) 251
- [4] S. I. Krasheninnikov, A. S. Kukushkin, Sov. Tech. Phys. Lett. **14** (1988) 228
- [5] A. Loarte, et al., Phys. Rev. Lett., **83** (1999) 3657; S. I. Krasheninnikov, et al., Nucl. Fusion **27** (1987) 1805
- [6] G. W. Pacher, et al., this conference.